

# Systemic Exosomal Delivery of shRNA Minicircles Prevents Parkinsonian Pathology

María Izco,<sup>1</sup> Javier Blesa,<sup>2</sup> Martin Schleeß,<sup>3</sup> Marco Schmeer,<sup>3</sup> Riccardo Porcari,<sup>4</sup> Raya Al-Shawi,<sup>4,5</sup> Stephan Ellmerich,<sup>4</sup> María de Toro,<sup>6</sup> Chris Gardiner,<sup>7</sup> Yiqi Seow,<sup>8</sup> Alejandro Reinares-Sebastian,<sup>2</sup> Raquel Forcen,<sup>1</sup> J. Paul Simons,<sup>4,5</sup> Vittorio Bellotti,<sup>4</sup> J. Mark Cooper,<sup>9</sup> and Lydia Alvarez-Erviti<sup>1,9</sup>

<sup>1</sup>Laboratory of Molecular Neurobiology, Center for Biomedical Research of La Rioja (CIBIR), Logroño 26006, La Rioja, Spain; <sup>2</sup>HM CINAC, Hospital Universitario HM Puerta del Sur, Mostoles 28938, Madrid, Spain; <sup>3</sup>PlasmidFactory GmbH & Co. KG, Bielefeld 33607, Germany; <sup>4</sup>Wolfson Drug Discovery Unit, Centre for Amyloidosis and Acute Phase Proteins, University College London, London NW3 2PF, UK; <sup>5</sup>Centre for Biomedical Science, Division of Medicine, University College London, London NW3 2PF, UK; <sup>6</sup>Genomics and Bioinformatics Core Facility, Center for Biomedical Research of La Rioja (CIBIR), Logroño 26006, La Rioja, Spain; <sup>7</sup>Department of Haematology, University College London, London NW3 2PF, UK; <sup>8</sup>Molecular Engineering Laboratory, Biomedical Sciences Institutes, A\*STAR, Singapore 138668, Singapore; <sup>9</sup>Department of Clinical Neuroscience, Institute of Neurology, University College London, London NW3 2PF, UK

**The development of new therapies to slow down or halt the progression of Parkinson's disease is a health care priority. A key pathological feature is the presence of alpha-synuclein aggregates, and there is increasing evidence that alpha-synuclein propagation plays a central role in disease progression. Consequently, the downregulation of alpha-synuclein is a potential therapeutic target. As a chronic disease, the ideal treatment will be minimally invasive and effective in the long-term. Knockdown of gene expression has clear potential, and siRNAs specific to alpha-synuclein have been designed; however, the efficacy of siRNA treatment is limited by its short-term efficacy. To combat this, we designed shRNA minicircles (shRNA-MCs), with the potential for prolonged effectiveness, and used RVG-exosomes as the vehicle for specific delivery into the brain. We optimized this system using transgenic mice expressing GFP and demonstrated its ability to downregulate GFP protein expression in the brain for up to 6 weeks. RVG-exosomes were used to deliver anti-alpha-synuclein shRNA-MC therapy to the alpha-synuclein preformed-fibril-induced model of parkinsonism. This therapy decreased alpha-synuclein aggregation, reduced the loss of dopaminergic neurons, and improved the clinical symptoms. Our results confirm the therapeutic potential of shRNA-MCs delivered by RVG-exosomes for long-term treatment of neurodegenerative diseases.**

## INTRODUCTION

Parkinson's disease (PD) is the second most common neurodegenerative disorder worldwide, but effective disease-modifying treatments are still lacking.<sup>1</sup> The primary cause of PD in the majority of patients is not known; however, various genetic mutations have been used to define the potential disease mechanisms involved. A number of mutations and duplications of the alpha-synuclein gene (SNCA) are a known cause of familial PD, and genome-wide association studies have highlighted the SNCA locus as a potential PD risk factor.<sup>2</sup> When combined with the observation that alpha-synuclein aggregates are a predomi-

nant feature of Lewy bodies in all PD patients, it is clear that alpha-synuclein plays an important role in PD pathogenesis.<sup>3</sup> More recently, alpha-synuclein aggregation has been shown to be transmitted from pathologically affected neurons to healthy unaffected neurons;<sup>4,5</sup> critically, the injection of alpha-synuclein fibrils into the striatum of normal mice is sufficient to recapitulate important clinical and pathological features of PD.<sup>6</sup> Consequently, the central role of alpha-synuclein in PD pathogenesis suggests that strategies to decrease the expression of neuronal alpha-synuclein levels are an attractive approach for the prevention and treatment of PD.

Gene therapy is a promising tool for the treatment of PD. The downregulation of alpha-synuclein levels using small interfering RNA (siRNA)<sup>7</sup> or short hairpin RNA (shRNA) delivered by adeno-associated virus (AAV)<sup>8</sup> in the CNS decreased alpha-synuclein aggregates and motor deficit in transgenic or toxin-based models of PD. However, one of the major challenges is designing a system that will readily deliver molecules to the brain and modify the disease by altering gene expression for prolonged periods, preferably in delivery vehicles that are not hindered by immune inhibition, such as with AAV.<sup>9</sup> We developed modified exosomes, which specifically target the brain, by placing a brain-targeting peptide (rabies virus glycoprotein [RVG] peptide) on the exterior surface of the exosome. These RVG-modified exosomes loaded with siRNAs and injected into the tail vein safely delivered the siRNAs to the brain, causing an effective knockdown of BACE1<sup>10</sup> and alpha-synuclein<sup>11</sup> protein throughout the brain. While successful, the half-life of siRNAs *in vivo* is relatively short, and the treatment of chronic diseases would require longer term gene silencing. Plasmids expressing a shRNA are better for longer term gene silencing;

Received 13 September 2018; accepted 14 August 2019;  
<https://doi.org/10.1016/j.ymthe.2019.08.010>

**Correspondence:** Lydia Alvarez-Erviti, PhD, Laboratory of Molecular Neurobiology, Center for Biomedical Research of La Rioja (CIBIR), Logroño 26006, La Rioja, Spain.

**E-mail:** [laerviti@riojasalud.es](mailto:laerviti@riojasalud.es)

however, conventional plasmids are relatively large and have been resistant to electroporation into exosomes (unpublished data). Minicircles (MCs), however, are double-stranded DNA vectors that contain the transgene expression cassette without additional bacterial sequences,<sup>12</sup> making them smaller but favoring higher transgene expression for longer periods<sup>13</sup> and, therefore, have the potential to deliver greater target depletion for a longer period of time.<sup>13</sup> In this way, MCs are excellent candidates for use with RVG-exosomes to deliver shRNAs and would represent an ideal combination for a disease-modifying therapy for PD and other neurodegenerative diseases.

In this study, we demonstrated that shRNA-MC constructs can be readily delivered to the CNS by RVG-exosomes and decrease target gene expression for prolonged periods. More specifically, we have now been able to demonstrate a decrease in alpha-synuclein expression in the brain of a mouse model of PD, decreasing the level of alpha-synuclein aggregation, reducing the loss of dopaminergic neurons in the substantia nigra pars compacta (SNc), and improving the clinical symptoms. These results confirm the potential of shRNA-MC RVG-exosome therapy to induce long-term downregulation of protein expression in the brain and could be further developed as an effective PD therapy. In principle, this novel approach can be applied to other neurodegenerative diseases.

## RESULTS

### Optimization and Validation of shRNA-MC RVG-Exosomes

RVG-exosomes were isolated from the conditioned media from primary dendritic cells transfected with RVG-Lamp2b.<sup>10</sup> Optimal conditions for loading the RVG-exosomes (3  $\mu$ g protein) with 1  $\mu$ g anti-GFP shRNA-MC constructs (Table S1) were evaluated using their efficacy at downregulating GFP expression in SH-SY5Y cells expressing GFP. The most efficient downregulation of GFP was obtained using electroporation, with electroporation buffer, at 400 V-125  $\mu$ F or 450 V-100  $\mu$ F, with the latter condition giving slightly greater GFP knockdown (Figure S1A). The size profile of the exosomes after electroporation was within normal limits (Figure S1B), and DNase protection assay confirmed that the shRNA-MCs were present inside exosomes after electroporation (Figure 1A; Figure S1C).

The efficiency of anti-GFP shRNA-MCs to downregulate GFP expression following different delivery methods was evaluated in SH-SY5Y cells expressing GFP, relative to actin protein levels (Figure 1B). Relative to controls, cells transfected with 1  $\mu$ g GFP shRNA-MCs using X-tremeGENE HP Transfection Reagent demonstrated a 47% decrease in GFP protein (TR in Figure 1B,  $p = 0.046$ ). Cells treated with 3  $\mu$ g RVG-exosomes electroporated with 1  $\mu$ g anti-GFP shRNA-MCs purified by centrifugation alone demonstrated a 45% decrease in GFP (Exo in Figure 1B,  $p = 0.046$ ), and this was similar for cells treated with RVG-exosomes loaded with GFP shRNA-MCs following DNase treatment to destroy un-encapsulated DNA (DNase in Figure 1B, 50%,  $p = 0.046$ ).

To investigate the ability of shRNA-MC RVG-exosomes to downregulate gene expression in the CNS, we evaluated the intravenous

(i.v.) injection of 150  $\mu$ g RVG-exosomes electroporated with two different anti-GFP shRNA-MC concentrations (100  $\mu$ g or 150  $\mu$ g MCs) into a transgenic mouse overexpressing EGFP. After 30 days, GFP protein levels were significantly decreased in the olfactory bulb and midbrain regions, and the decrease in GFP was always higher with 150  $\mu$ g MC-loaded exosomes (Figures S2A and S2B). Extraction of the anti-GFP shRNA-MC construct from the electroporated RVG-exosomes (150  $\mu$ g shRNA-MCs with 150  $\mu$ g RVG-exosomes) revealed a 19%  $\pm$  5% recovery of the shRNA-MC DNA in the RVG-exosomes (30  $\mu$ g shRNA-MCs/150  $\mu$ g exosomes), as quantified by nanodrop analysis.

Our results demonstrated that anti-GFP shRNA-MCs can be successfully loaded into RVG-exosomes, which can downregulate GFP protein levels *in vitro* for at least 30 days in selected brain regions after i.v. administration.

### Evaluation of Alpha-Synuclein Downregulation by shRNA-MC RVG-Exosomes

An anti-alpha-synuclein shRNA-MC construct was generated using a sequence that targets both mouse and human alpha-synuclein mRNA (Table S1) based on previous siRNA downregulation studies.<sup>11</sup> RVG-exosomes (3  $\mu$ g) were loaded with anti-alpha-synuclein shRNA-MC construct (1  $\mu$ g) using the optimized conditions used earlier, and their ability to downregulate alpha-synuclein protein was evaluated in SH-SY5Y cells overexpressing S129D alpha-synuclein. Relative to controls, S129D alpha-synuclein protein levels were significantly decreased 72 h after lipofection with anti-alpha-synuclein shRNA-MCs (MC-TR in Figure 1C; 1  $\mu$ g, decreased by 44%,  $p = 0.009$ ), with the shRNA alpha-synuclein parental plasmid (Plasmid-TR in Figure 1C; 1  $\mu$ g, decreased 41.3%,  $p = 0.014$ ) or with the previously used anti-alpha-synuclein siRNA (siRNA-TR in Figure 1C; 100 nM decreased 37%,  $p = 0.009$ ).<sup>11</sup> Alpha-synuclein protein levels were decreased to a similar extent after incubation with 3  $\mu$ g RVG-exosomes containing either alpha-synuclein siRNA (siRNA Exo; 100 nM, decreased 48.3%,  $p = 0.025$ ) or anti-alpha-synuclein shRNA-MCs (MC Exo; 1  $\mu$ g, decreased 47%,  $p = 0.014$ ), as shown in Figure 1C, suggesting that delivery by RVG-exosomes to SH-SY5Y cells was at least as efficient as transfection.

The efficacy of the i.v. delivery of RVG-exosomes containing anti-alpha-synuclein shRNA-MCs to downregulate alpha-synuclein *in vivo* was studied using a transgenic mouse model expressing the phosphomimic human S129D alpha-synuclein-HA under the prion promoter.<sup>11</sup> This model exhibits alpha-synuclein aggregates throughout the brain from 3 months of age. 10- to 14-week-old transgenic mice received i.v. injections of 150  $\mu$ g RVG-exosomes electroporated with 150  $\mu$ g anti alpha-synuclein shRNA-MCs ( $n = 10$ ) or 150  $\mu$ g RVG-exosomes loaded with 150  $\mu$ g anti-GFP shRNA-MCs as a control group ( $n = 5$ ) and were compared with mice injected with vehicle alone ( $n = 10$ ). Mice were sacrificed 45 days after injection and were evaluated for alpha-synuclein mRNA and protein levels. Administration of anti-alpha-synuclein shRNA-MC RVG-exosomes resulted in the downregulation of S129D alpha-synuclein-HA mRNA levels in

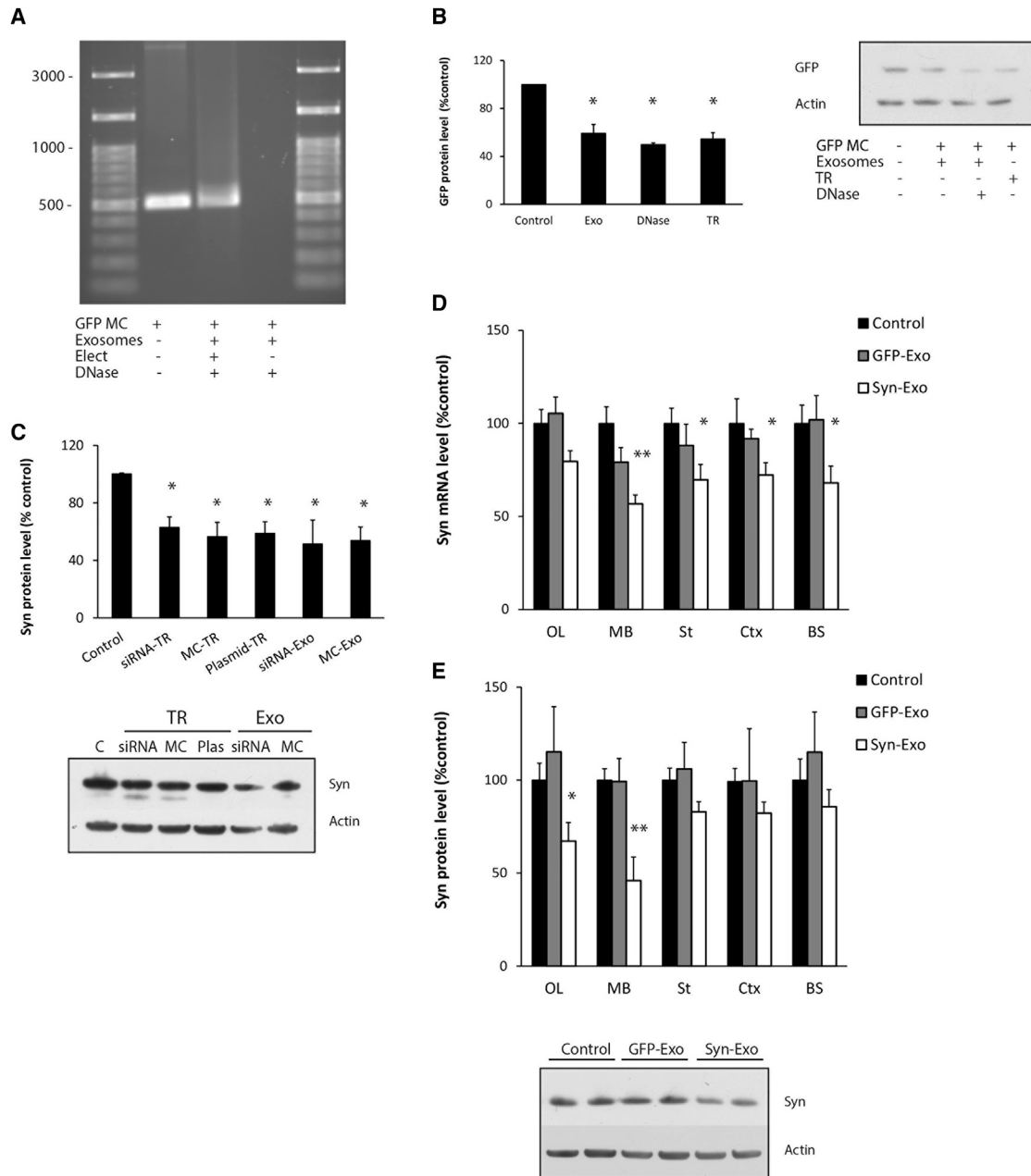


**Figure 1. Optimization of Exosomal Loading and Influence on Alpha-Synuclein Levels in SH-SY5Y Cells and in the Brain of S129D Alpha-Synuclein Transgenic Mice**

(A) Agarose gel electrophoresis of anti-GFP shRNA-MC DNA (GFP MC) or DNA isolated from GFP MCs incubated with RVG-exosomes with (Elect) or without (No elect) electroporation followed by DNase treatment. (B) GFP levels in SH-SY5Y cells overexpressing GFP after delivery of anti-GFP shRNA-MCs by 3  $\mu$ g RVG-exosomes after centrifugation (Exo), after centrifugation and treatment with DNase (DNase), or after transfection of 1  $\mu$ g GFP shRNA-MC using XtremeGENE Transfection Reagent (TR) (n = 4). GFP and actin protein levels were quantified by western blot. Values are expressed as mean  $\pm$  SEM. (C) SH-SY5Y cells overexpressing S129D alpha-synuclein were transfected with 100 nM anti-alpha-synuclein siRNAs (siRNA), 1  $\mu$ g anti-alpha-synuclein shRNA MCs (MC), or anti-synuclein shRNA plasmid (Plas) or were treated with 3  $\mu$ g RVG-exosomes (Exo) electroporated with 100 nM anti alpha-synuclein siRNAs (siRNA), or 1  $\mu$ g anti-alpha-synuclein shRNA-MCs (MC). Quantitation of alpha-synuclein protein levels normalized to control cells and a typical western blot are shown. Data are expressed as mean  $\pm$  SEM (n = 3). \*p < 0.05; \*\*p < 0.01, non-parametric Kruskal-Wallis test, statistical analyses compared with untreated control group. (D and E) S129D alpha-synuclein transgenic mice were treated with 150  $\mu$ g RVG-exosomes containing anti-GFP (GFP-Exo) or anti-alpha-synuclein shRNA-MCs (Syn-Exo). Olfactory bulb (OL), midbrain (MB), striatum (St), cortex (Ctx), and brainstem (BS) samples were analyzed for (D) alpha-synuclein mRNA by qPCR and (E) protein levels by western blot. A typical western blot of the midbrain is shown. Data are expressed as mean  $\pm$  SEM (n = 10). \*p < 0.05; \*\*p < 0.01, one-way ANOVA, statistical analyses compared with untreated control group.

all regions studied, which were significantly lower in the midbrain (decreased by 45%,  $p = 0.001$ ), cortex (decreased by 28%,  $p = 0.043$ ), striatum (decreased by 30%,  $p = 0.042$ ), and brainstem (decreased by 32%,  $p = 0.04$ ), but there were no consistent changes in the group treated with anti-GFP shRNA-MC RVG-exosomes (Figure 1D). In the group treated with alpha-synuclein shRNA-MCs, the S129D alpha-synuclein-HA protein levels were lower than those of the controls in all regions studied, and these were significantly lower in olfactory bulb (decreased 33%,  $p = 0.034$ ) and midbrain (decreased 54%,  $p = 0.003$ ) (Figure 1E), confirming the potential of this therapy for longer term downregulation of alpha-synuclein levels in the CNS.

The serum levels of tumor necrosis factor alpha (TNF- $\alpha$ ), interferon (IFN)- $\gamma$ , interleukin (IL)-6, and IFN- $\gamma$ -induced protein 10 (IP-10) in the alpha-synuclein- or GFP-shRNA-MC RVG-exosome-treated mice 45 days post-treatment were not increased to levels indicating that they had induced immune activation and were not significantly different from those of the controls (Table S2).

#### Alpha-Synuclein shRNA-MC RVG-Exosomal Therapy Prevents the Neurodegeneration in the Syn PFF Mouse Model of PD

While the *in vivo* RVG-exosome delivery of anti-alpha-synuclein shRNA-MC therapy was able to decrease brain alpha-synuclein protein levels over a prolonged period, it is important to identify whether this can influence the clinical, pathological, and degenerative changes typical of parkinsonism. The progressive alpha-synucleinopathy mouse model based on the intrastriatal injection of alpha-synuclein preformed fibrils (Syn PFFs) exhibits the progressive spread of alpha-synuclein aggregation, loss of dopaminergic neurons, and clinical defects affecting motor functions<sup>6</sup> and is ideal for evaluating the efficacy of this therapy on key clinical and pathological features associated with PD.

Initial studies that aimed to both establish the Syn PFF model and confirm the efficacy of the RVG-exosomally delivered anti-alpha-synuclein shRNA-MC therapy in this model were performed. 24 normal C57BL6/C3H mice received unilateral intrastriatal injections of murine alpha-synuclein PFFs. After 2 days, mice received *i.v.* injections of 150  $\mu$ g RVG-exosomes loaded with alpha-synuclein shRNA-MCs (150  $\mu$ g;  $n = 8$ ) or 150  $\mu$ g RVG-exosomes loaded with anti-GFP shRNA-MCs (150  $\mu$ g;  $n = 8$ ) or an *i.v.* injection of vehicle (glucose 5%;  $n = 8$ ). Mice were sacrificed 30 days after the treatment.

After 30 days, in the Syn-PFF-injected mice, there were no detectable changes in alpha-synuclein mRNA levels in the ipsilateral (Figure 2A) or contralateral (Figure 2C) brain regions relative to control mice. There was a significant increase in alpha-synuclein protein levels in the striatum, reflecting alpha-synuclein aggregation (Figure 2B), which was observed as S129 phospho-alpha-synuclein-positive neurites in striatum and inclusions in the midbrain (Figure S3), consistent with alpha-synuclein aggregation as previously reported.<sup>6</sup> In the Syn-PFF-injected mice, 30 days after treatment with anti-alpha-synuclein shRNA-MC RVG-exosome therapy, there was evidence that alpha-synuclein mRNA levels remained downregulated in the

ipsilateral midbrain (decreased by 29%, not significant), striatum (decreased by 36%,  $p = 0.046$ ), and cortex (decreased by 29%, not significant) relative to control but unaffected in the mice treated with RVG-exosomes loaded with anti-GFP shRNA-MCs (Figure 2A). At this time point, the RVG-exosome alpha-synuclein shRNA-MC therapy was associated with a decrease in alpha-synuclein protein levels in all 3 ipsilateral brain regions analyzed (Figure 2B); in particular, the significant increase in alpha-synuclein levels in the striatum with Syn PFF injection was reduced to values approaching those of the controls. However, with RVG-exosome anti-GFP shRNA-MC therapy, alpha-synuclein levels were similar to those of PFF-treated mice, confirming the specificity of the alpha-synuclein shRNA-MCs (Figure 2B). The S129 phospho-alpha-synuclein-positive inclusions evident in the midbrain of the Syn-PFF-injected mice (Figure S3) were also present in the GFP-shRNA-MC-treated (Figure S3) and the alpha-synuclein-shRNA-MC-treated mice, although this preliminary study suggested that aggregates were mildly lower in the latter (decreased 20%, not significant; Figure S3).

In a second cohort of mice, the RVG-exosome anti-alpha-synuclein shRNA-MC therapy was extended to 90 days after Syn PFF injections to explore the impact of the therapy on the neurodegenerative process. The mice were treated as described earlier, except a second therapeutic *i.v.* injection was administered after 45 days, and the mice were analyzed 90 days after Syn PFF injection. At 90 days, striatal Syn PFF injections were associated with S129 phospho-alpha-synuclein-positive inclusions in the SNc; the frontal, somatosensory, and somatomotor cortex; the amygdala; and the striatum (Figures 3A and 3B)—inclusions that were not observed in control mice (data not shown), consistent with the PFF induction and spread of alpha-synuclein aggregation. After 90 days of the treatment with RVG-exosomes containing anti-alpha-synuclein shRNA-MC therapy, there was a significant decrease in phospho-synuclein-positive aggregates in the frontal (decreased 58%  $p = 0.045$ ), somatosensory (decreased 65%  $p = 0.02$ ), and somatomotor (decreased 80%  $p = 0.014$ ) cortex, as well as the amygdala (decreased 37%  $p = 0.048$ ) and SNc (decreased 37%  $p = 0.046$ ) (Figures 3A–3C); however, in the striatum, the change was not significant. After 90 days, the alpha-synuclein mRNA levels remained lower in all 3 brain regions analyzed in both the ipsilateral and contralateral parts of the brain (Figures 4A–4B). This reduction was statistically significant in the ipsilateral midbrain (decreased 37% compared to controls,  $p = 0.039$ ) and cortex (decreased 47% compared to controls,  $p < 0.001$ ), and in the contralateral midbrain (decreased 42% compared to controls,  $p = 0.027$ ) (Figures 4A and 4B). The prolonged decrease in alpha-synuclein mRNA levels in the contralateral regions were associated with lower levels of alpha-synuclein protein in all 3 regions, and this was statistically significant in the midbrain (decreased 60% compared to controls,  $p = 0.033$ ) and cortex (decreased 55% compared to controls,  $p = 0.039$ ) (Figure 4D). Of the ipsilateral regions, however, only alpha-synuclein protein in the midbrain remained significantly decreased (decreased 54% compared to controls,  $p = 0.043$ ). In the striatum and cortex, the alpha synuclein protein levels were similar to those of controls (Figure 4D); this may reflect the alpha-synuclein aggregation evident in the ipsilateral brain

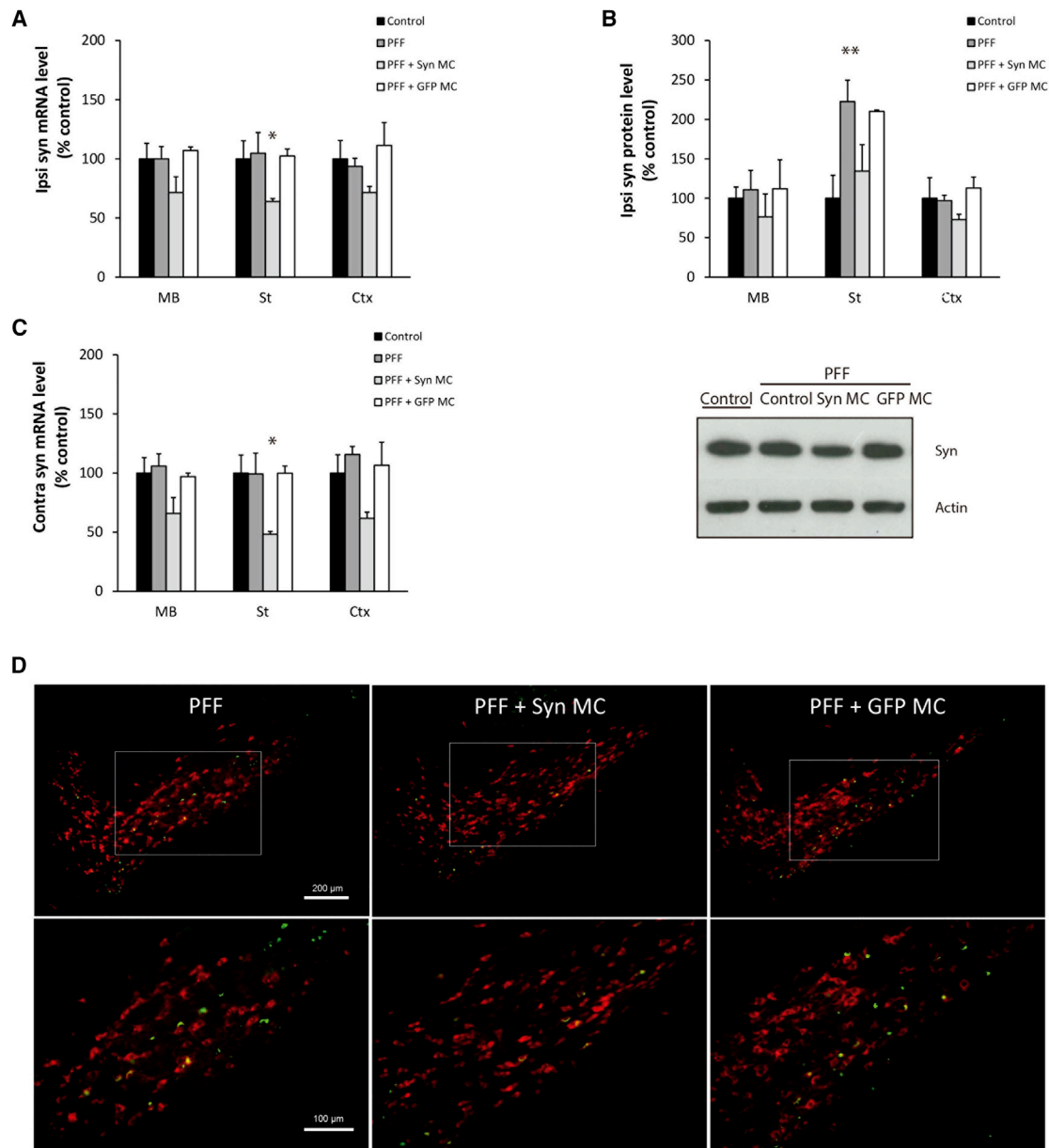


**Figure 2. Effect of Anti-alpha-synuclein shRNA-MC RVG-Exosome Treatment 30 days after Administration in PFF-Treated Mice**

Normal C57BL6/C3H F1 mice intrastriatally injected with alpha-synuclein PFFs (PFF) were treated with i.v. injections of 150 μg RVG-exosomes electroporated with 150 μg anti-alpha-synuclein shRNA-MC (PFF + Syn MC) or 150 μg anti-GFP shRNA-MC (PFF + GFP MC) for 30 days. (A and B) Analyses of alpha-synuclein (A) mRNA expression and (B) protein levels normalized to actin in ipsilateral midbrain (MB), striatum (St), and cortex (Ctx). Values are expressed as mean ± SEM (n = 5). Typical western blot of the midbrain is shown. (C) Analyses of alpha-synuclein mRNA levels normalized to actin in the contralateral midbrain (MB), striatum (St), and cortex (Ctx). Data are expressed as mean ± SEM (n = 4). \*p < 0.05; \*\*p < 0.01, non-parametric Kruskal-Wallis test. (D) Immunofluorescent staining of midbrain sections with antibodies to S129 phospho-alpha-synuclein (green) and tyrosine hydroxylase (red). Scale bars, 200 μm (top) and 100 μm (bottom).

(Figures 3A and 3B), which may be more resistant to the effects of shRNA therapy.

The mice injected with Syn PFFs demonstrated a unilateral loss of dopaminergic innervation with a decrease in tyrosine hydroxylase (TH) staining in the anterior, medium, and posterior striatum of

21% (p < 0.001), 41% (p < 0.001), and 56% (p < 0.001), respectively (Figure 5A). Immunostaining for dopamine transporter (DAT) confirmed the loss of dopaminergic innervation with a decreased staining in the anterior, medium, and posterior striatum of 13% (p = 0.025), 27% (p < 0.001), and 48% (p < 0.001), respectively (Figures S5A and S5B). Stereological evaluation of TH-positive staining

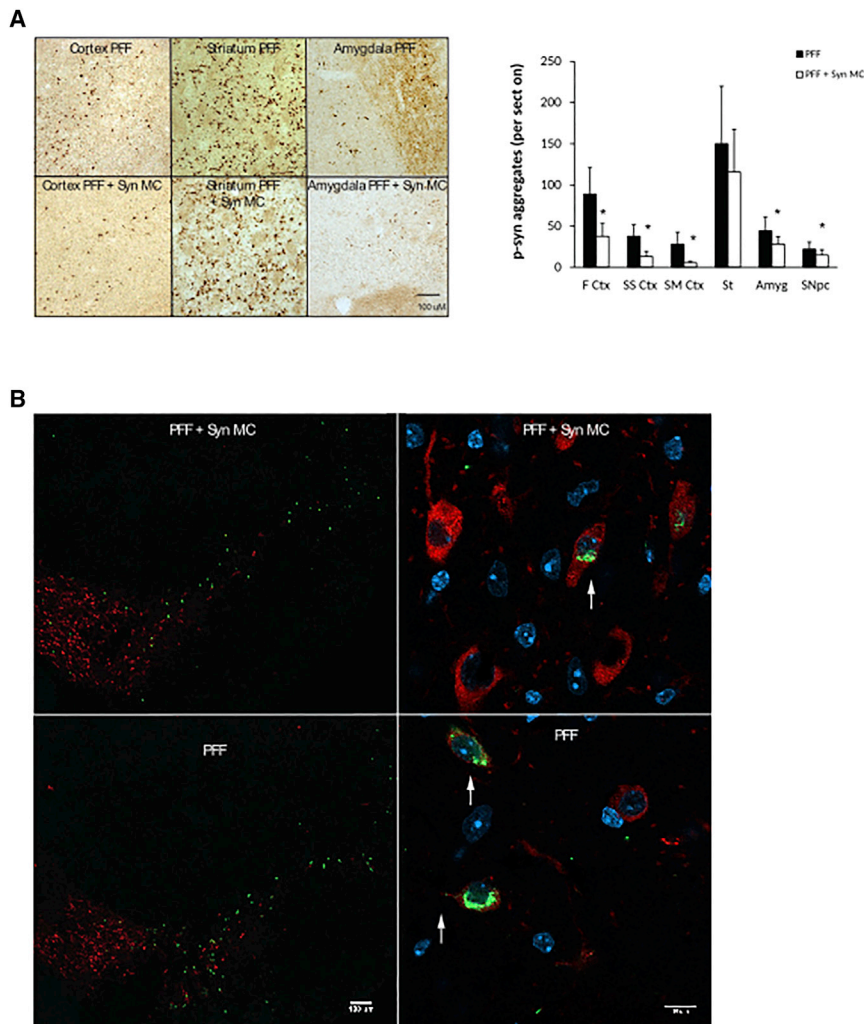


**Figure 3. Influence of 90-Day Anti-alpha-synuclein shRNA-MC RVG-Exosome Treatment on Alpha-Synuclein Aggregation**

(A) Brain sections were stained for S129 phospho-synuclein, and the number of positive aggregates per section in the frontal cortex (F Ctx), somatosensory cortex (SS Ctx), somatomotor cortex (SM Ctx), striatum (St), amygdala (Amyg), and substantia nigra (SNc) were quantified. Typical immunohistochemical images of frontal cortex, striatum, and amygdala stained for S129 phospho-alpha-synuclein are shown. Data are expressed as mean  $\pm$  SEM (n = 8). \*p < 0.05, non-parametric Kruskal-Wallis test. (B) Immunofluorescent staining of midbrain sections with antibodies to S129 phospho-alpha-synuclein (green) and tyrosine hydroxylase (red). Magnified regions of the SNc are shown on the right; arrows indicate alpha-synuclein aggregates. Scale bars, 100  $\mu$ m (left) and 10  $\mu$ m (right).

shRNA-MC RVG-exosome therapy being indistinguishable from that of the control mice (Figures 5C and 5D).

To assess whether anti-alpha-synuclein shRNA-MC RVG-exosome therapy affects the inflammatory response, brain sections from mice 90 days after Syn PFF injection were stained with anti-Iba1 antibodies and assessed for the number and morphology of positive cells. Activated microglia are usually increased in number and size with shortened and clumpy processes and can be qualitatively evaluated with the Colburn scale (Table S6). Striatal injection of Syn PFF was associated with a modest non-significant increase in the number and average size of Iba1-positive cells in those areas exhibiting S129 phospho-alpha-synuclein inclusions (Figures S4A–S4D). The qualitative analysis of microglia using the Colburn scale suggested that microglial cells were demonstrating features indicating mild activation at 90 dpi (score  $\geq$  1) in all the areas analyzed (Figure S4E), whereas the Colburn scores approached the control levels following anti-alpha-synuclein shRNA-MC RVG-exosomal treatment.

To evaluate the impact of repeated therapeutic applications on inflammatory markers, TNF- $\alpha$ , IFN- $\gamma$ , IL-4, IL-5, IL-6, and IL-12p70 levels were analyzed in serum after alpha-synuclein shRNA-MC RVG-exosome treatment. The levels of these cytokines were not significantly elevated in either the Syn-PFF- or the Syn-PFF- and RVG-exosome shRNA-MC-treated mice (Table S3). This confirms that two doses of anti-alpha-synuclein shRNA-MC RVG-exosome therapy did not activate the immune response in mice, nor did they have off-target effects assessed by transcriptomic analysis compared to Syn PFF mice (Table S4).

To analyze whether the prolonged downregulation of alpha-synuclein associated with this therapy had any detrimental effects, we studied 3

neurons in the midbrain demonstrated that Syn-PFF-injected mice had a unilateral 30% loss of dopaminergic neurons in the SNc (p = 0.002) (Figure 5B). Motor performance was evaluated at 30, 60, and 90 days using the negative geotaxis and wire hanging tests. In agreement with previous studies,<sup>6</sup> after 90 days, the performance of the Syn-PFF-treated mice was compromised significantly on the negative geotaxis test (p = 0.047) and the wire hanging test (p = 0.036) (Figures 5C and 5D).

The anti-alpha-synuclein shRNA-MC RVG-exosomal treatment reduced the dopaminergic neuronal loss associated with Syn PFF treatment, with levels similar to those of the controls (75% inhibition of cell loss relative to Syn PFF mice, p = 0.028) (Figure 5B). This was associated with a significant protection against the Syn-PFF-induced loss of dopaminergic terminals in the striatum (Figure 5A; Figures S5A and S5B). These improvements in pathology were associated with improved clinical parameters at 90 days, with the performance of the Syn-PFF-treated mice that received the anti-alpha-synuclein

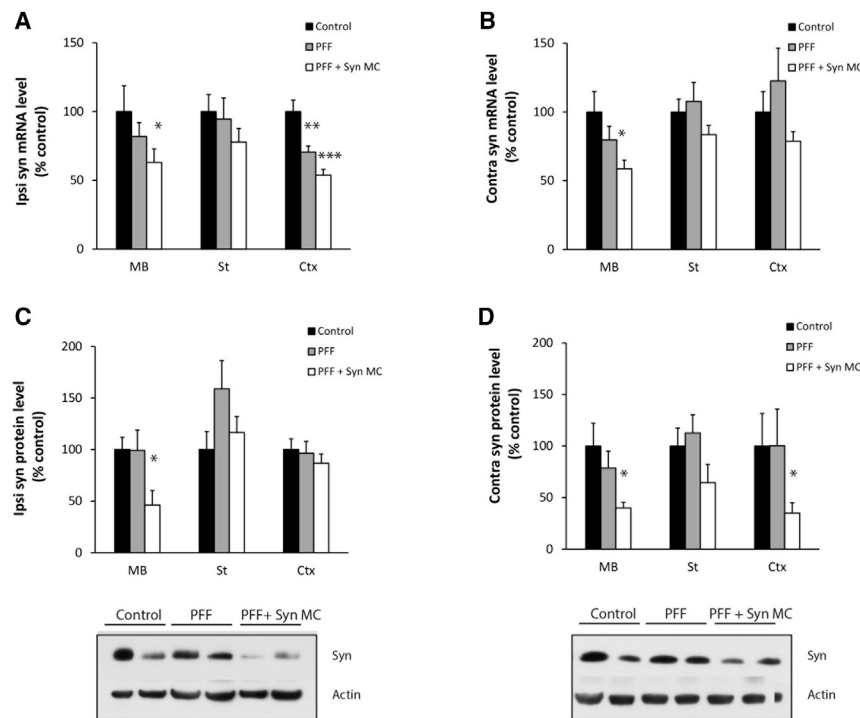


**Figure 4. Effect of 90-Day Anti-alpha-synuclein shRNA-MC RVG-Exosome Treatment on Alpha-Synuclein mRNA and Protein**

(A–D) Quantitation of alpha-synuclein (A and B) mRNA levels and (C and D) protein levels in the (A and C) ipsilateral and (B and D) contralateral midbrain (MB), striatum (St), and cortex (Ctx) from alpha-synuclein PFF-treated mice (PFF) after 90 days following anti-alpha-synuclein shRNA-MC RVG-exosome treatment (PFF + Syn MC). mRNA and protein levels were normalized to actin; typical western blots of the midbrain are shown. Data are expressed as mean  $\pm$  SEM (n = 10). \*p < 0.05; \*\*p < 0.01; \*\*\*p < 0.001, one-way ANOVA, statistical analyses compared with control group.

siRNAs<sup>11,14,16</sup> or plasmids<sup>16</sup> that required re-administration every few days. This longer downregulation represents a clear clinical advantage for the prevention and treatment of chronic neurodegenerative diseases.

Alpha-synuclein is increasingly recognized as an important target for PD therapy, with a suggestion that its downregulation may delay or halt disease progression.<sup>17</sup> To date, several therapeutic approaches designed to combat the progressive increase in alpha-synuclein aggregates in PD have been reported.

These include strategies to prevent its aggregation, such as the use of intrabodies<sup>18</sup> or hsp70 overexpression,<sup>19</sup> or to promote the removal of alpha-synuclein by immunization.<sup>20,21</sup> Weekly intraperitoneal administration of alpha-synuclein immunotherapy for 30 days has been reported to decrease alpha-synuclein aggregates, improve motor behavior, and reduce dopaminergic cell death in the alpha-synuclein PFF model.<sup>21</sup> However, the immunotherapy approach has some important issues to resolve regarding the antibody brain penetration, the timing of intervention in the course of the disease, and the targeting of the extracellular alpha-synuclein. Moreover, LRRK2 antisense oligonucleotides have also been reported to reduce alpha-synuclein aggregation and cell death in this model;<sup>22</sup> however, this treatment required intraventricular administration and high doses of the gene therapy molecule, and its influence was relatively local.

The approach we report here to decrease alpha-synuclein levels by exosomal delivery of shRNA-MCs has the advantage that it is minimally invasive and acts on the intracellular protein levels and could lead to a decrease in monomeric protein, preventing its aggregation or post-translational modification. Previous studies reported dopaminergic alpha-synuclein downregulation using the intra-cerebral administration of AAV2 viral vectors and confirmed the therapeutic potential of this intervention in transgenic<sup>23</sup> and toxin-based<sup>8</sup> models of PD. In agreement with all these reports, our results confirmed that, in a model demonstrating the spread of alpha-synuclein aggregation, loss of DA neurons, and movement defects, decreasing alpha-synuclein expression was an effective therapy, strengthening this approach as a

groups of control mice sham-injected intrastrially and treated with 2 doses of RVG-exosomes loaded with alpha-synuclein shRNA-MCs, RVG-exosomes loaded with anti-GFP shRNA-MCs, or vehicle. Mice were analyzed 100 days after the first i.v. treatment. The RVG-exosome alpha-synuclein shRNA-MC therapy was associated with a significant decrease in alpha-synuclein mRNA and protein levels in midbrain, which was not apparent in the RVG-exosome anti-GFP shRNA-MC therapy (Figure S6A). There was no evidence that the decrease in alpha-synuclein levels was associated with detectable changes in: striatal dopaminergic innervation (Figure S6B), the number of TH-positive staining neurons in the midbrain (Figure S6C), or the results of the wire hanging test of motor performance (Figure S6D).

## DISCUSSION

In this study, we have demonstrated the potential of shRNA-MC RVG-exosomal therapy to induce the long-term downregulation of targeted genes in the CNS. More specifically, we have been able to use this therapeutic approach to prevent dopaminergic cell death and motor abnormalities in a progressive mouse model of PD. Previous studies confirmed that i.v. injection of un-targeted exosomes,<sup>10</sup> empty exosomes,<sup>10</sup> or exosomes loaded with inactive modified siRNA<sup>11</sup> did not significantly affect mRNA or protein expression in the brain. The present results confirm the capability of RVG-exosomes to deliver nucleic acids safely and specifically to the CNS in agreement with previous reports.<sup>11,14,15</sup> The exosomal delivery of MCs expressing shRNA now extends the duration of knockdown achieved to over 7 weeks, compared to previous strategies using

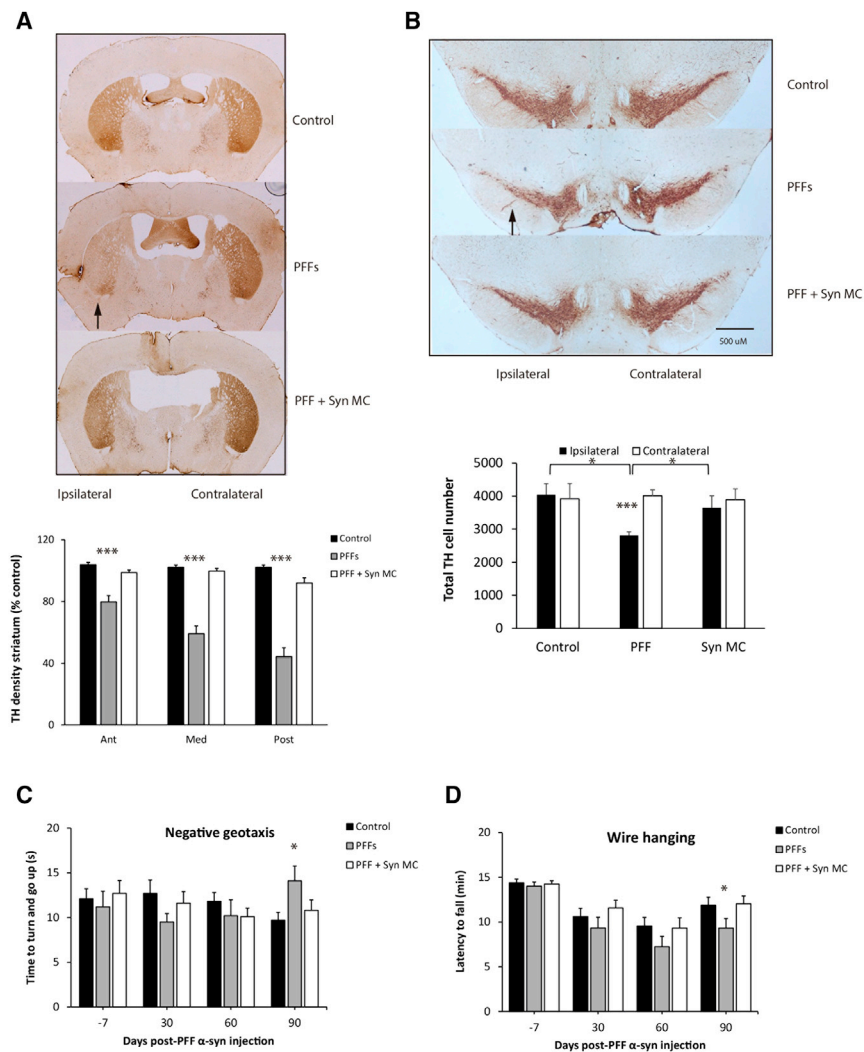


**Figure 5. Anti-alpha-synuclein shRNA-MC Delivery by RVG-Exosomes Reduces the Dopaminergic Denervation, Dopaminergic Neuronal Loss, and Motor Abnormalities Caused by Intrastratial Injection of Alpha-Synuclein PFFs**

(A) TH immunoreactivity was analyzed in coronal sections of the forebrain from: control mice, mice 90 days after alpha-synuclein PFF treatment alone (PFFs, ipsilateral striatum, black arrow), and following anti-alpha-synuclein shRNA-MC RVG-exosome treatment (PFF + Syn MC). Striatal TH was quantified by optical density in the ipsilateral sections normalized to the contralateral striatum. (B) Quantitation of nigral dopaminergic neurons on each side of the brain by unbiased stereology. Data are expressed as mean  $\pm$  SEM (n = 8). \*p < 0.05; \*\*\*p < 0.001, non-parametric Kruskal-Wallis test, statistical analyses compared with untreated control group. Clinical evaluations of the influence of alpha-synuclein PFF intrastratial injection (PFFs) and treatment with alpha-synuclein shRNA-MC RVG-exosomes (PFF + Syn MC). (C and D) As indicated here, (C) negative geotaxis and (D) wire hanging tests were performed in a comparison to control mice. Data are expressed as mean  $\pm$  SEM (n = 18). \*p < 0.05, one-way ANOVA, statistical analyses compared with untreated control group. Scale bars, 500  $\mu$ m.

alpha-synuclein, especially if only mildly decreased. The degree of alpha-synuclein downregulation may be a critical factor in determining any detrimental effects, and care may be required to obtain alpha-synuclein reduction enough to halt or delay the neurodegenerative process but sufficient to maintain the normal function of the protein fundamental for neuronal function.

In this study, we used the alpha-synuclein PFF intrastratial injected mouse model, where the injection of the Syn PFFs has been shown to lead to the spread of Lewy body (LB)-like aggregates, dopaminergic cell death, and behavioral and motor changes.<sup>6</sup> The roles of neuroinflammation and glial cell activation in PD have gained increased attention in recent years, and they are now recognized as important features of PD pathogenesis.<sup>29</sup> In this study, we assessed the microglia immuno-reactivity in the Syn PFF model at the stage when intraneuronal alpha-synuclein inclusions were linked to dopamine (DA) neuron death and motor impairments. Our results demonstrated in the Syn PFF-treated mice, at 90 dpi, that there was evidence for modest microglia activation in the areas affected by alpha-synuclein pathology and that there was a tendency for this to decrease to control levels following RVG-exosome shRNA-MC therapy. Mild inflammatory changes in this model are in agreement with data recently described in a rat model involving intrastratial injection of Syn PFF;<sup>30</sup> these authors observed an increase in immunoreactivity during the initial accumulation of intracellular alpha-synuclein prior to dopaminergic cell death but a significant decrease in microglial immunoreactivity during the period

PD treatment. A clear advantage of the exosomal approach is that it enables a more widespread downregulation of alpha-synuclein within the brain, with aggregation decreasing in most regions analyzed. Moreover, the prolonged downregulation of alpha-synuclein levels allows fewer administrations that have economic and therapeutic benefits. Some studies have reported a 25%–50% loss of dopaminergic neurons over 21 days, associated with a dramatic 45%–85% reduction in alpha-synuclein and an associated inflammatory response.<sup>24,25</sup> However, other studies have reported a decrease in alpha-synuclein expression using AAV in toxic and transgenic models,<sup>8,23</sup> without an associated decrease in TH expression. These results have been supported in a recent study using transgenic mouse models treated with an i.v. injection of AAV9, delivered to the brain using focused ultrasound (FUS) in combination with microbubbles.<sup>26</sup> The lack of toxicity associated with downregulated alpha-synuclein levels reported in these studies, and confirmed in our experiments, could be related with a lower level of alpha-synuclein downregulation. Moreover, SNCA knockout mice<sup>27,28</sup> have a relatively mild phenotype that supports the potential redundancy of

of degeneration. They suggested that an increase in major histocompatibility complex (MHC) class II microglia may be a first-response mechanism to the initial accumulation of intracellular alpha-synuclein and that the RVG-exosome shRNA-MC therapy reduced alpha-synuclein aggregation and could decrease microglia activation.

Our strategy involved treating the animals immediately after induction of the pathological process and, therefore, at the start of the spread of the pathology, prior to the development of the degenerative process and resulting clinical symptoms. Consequently, the benefits we observed may be limited to therapies applied very early in the disease process; therefore, it is important to address whether it can influence disease progression after the appearance of the pathology and after the onset of motor symptoms, corresponding to the initial clinical stage of PD.

The results of this study highlight the *in vivo* therapeutic potential of the RVG exosomal delivery of MC constructs. The combination of shRNA-MCs to downregulate gene expression with the specific delivery by targeted exosomes is a potential treatment not only for PD but also for other neurodegenerative diseases (e.g., Alzheimer's disease and amyotrophic lateral sclerosis), as well as other tissue-specific pathologies potentially amenable to gene therapy. This new therapy will offer a completely different approach to therapy for these progressive neurodegenerative illnesses and, we hope, will change the lives of those who live with these conditions.

## MATERIALS AND METHODS

### Cell Culture

The human SH-SY5Y neuroblastoma cell line (American Type Culture Collection) clones constitutively expressing human S129D alpha-synuclein with a C-terminal hemagglutinin (HA) tag or GFP-alpha-synuclein were cultured using standard conditions.<sup>11</sup>

### Exosome Isolation

Murine dendritic cells were harvested from bone marrow and cultured ( $3 \times 10^6$  cells per well, 6 wells per plate) in DMEM with GlutaMAX (GIBCO-BRL),<sup>10</sup> 10% fetal calf serum (FCS) depleted of exosomes by centrifugation at  $120,000 \times g$  for 60 min, and penicillin/streptomycin supplemented with 10 ng/mL murine GM-CSF (MP Biomedicals). Cells were transfected after 4 days with 5  $\mu$ g RVG-Lamp2b plasmid and 5  $\mu$ L TransIT LT1 Transfection Reagent (Mirus Bio) as per the manufacturer's instructions. Cell-culture medium was changed on day 7. After 24 h, the medium was removed, exosomes were harvested by centrifugation at  $12,000 \times g$  for 30 min to remove cell debris, and the supernatant was centrifuged again at  $120,000 \times g$  for 1 h to pellet exosomes. Exosomes were resuspended in 0.1 M ammonium acetate with a 27G needle.

### Loading of RVG-Exosomes with shRNA-MC Constructs

To determine the optimal conditions to load exosomes with shRNA-MC constructs, 1  $\mu$ g shRNA-MCs (see [Supplemental Information](#) for details) and 3  $\mu$ g RVG-exosomes were mixed in 100  $\mu$ L electroporation buffer (1.15 mM potassium phosphate [pH 7.2], 25 mM KCl,

21% OptiPrep), PBS, or Minimum Essential Medium (MEM) and electroporated using 3 different settings (450 V, 100 mA; 450 V, 250 mA; and 400 V, 125 mA) in a 4-mm cuvette using a Bio-Rad Gene Pulser Xcell Electroporator. The exosome samples were treated with 1 U DNase (Promega) for 30 min at 37°C and purified by ultracentrifugation at  $120,000 \times g$  for 1 h. Exosomes were resuspended in RPMI medium.

### Exosome Analysis and shRNA-MC Content

Extracellular vesicle size distribution was assessed by nanoparticle tracker analysis using a NS500 instrument (Nanosight), as described previously.<sup>11</sup> To evaluate the quality and concentration of shRNA-MCs in RVG-exosomes following electroporation and DNase treatment, ultracentrifuge-purified exosomes were used to purify the shRNA-MC constructs using the QIAprep Spin Miniprep Kit. DNA was qualitatively analyzed by ethidium-bromide-stained agarose gel electrophoresis and quantified using NanoDrop (Thermo Fisher Scientific) spectrophotometry. The percentage of shRNA-MCs loaded into RVG-exosomes by electroporation was quantified by qPCR and compared to the same amount of shRNA-MCs not electroporated. The DNase protection assay involved incubation of the samples with 1 U DNase at 37°C for 30 min.

### Treatment of Cells with siRNAs, shRNA Plasmid, and shRNA MC

Cells were transfected with 100 nM siRNAs (see [Supplemental Information](#) for details) (Eurogentec), using HiPerfect Transfection Reagent (QIAGEN), or with 1  $\mu$ g alpha-synuclein shRNA plasmid or 1  $\mu$ g anti-GFP or anti-alpha-synuclein shRNA-MC using 1  $\mu$ L X-tremeGENE HP Transfection Reagent (Roche).

### Experimental Design

Normal male C57BL6/C3H F1 mice (8 to 9 weeks old) and male EGFP (C57BL/6-Tg(CAG-EGFP)131Osb/LeySopJ) mice (8 to 10 weeks old) were purchased from Charles River Laboratories. Male S129D alpha-synuclein transgenic mice (10 to 14 weeks old)<sup>11</sup> were generated at University College London.

Normal C57BL6/C3H F1 (8- to 9-week-old) mice received an injection of sonicated murine alpha-synuclein PFFs (5  $\mu$ g) into the dorsal striatum as previously described.<sup>6</sup> All animal experiments were designed to minimize the suffering and pain of the animals and were conducted according to the NIH Guide for the Care and Use of Laboratory Animals. Sample size was calculated using an online program (<http://powerandsamplesize.com/Calculators/Compare-k-Means/1-Way-ANOVA-Pairwise>). All animals were randomly distributed to the cages by a technician of the animal facilities, and before any procedure, the cages were randomized to each group by a person not involved in the study. All the *in vivo* experiments were blinded, and the investigators responsible for data collection and analysis were blinded. The experiments with the EGFP and the S129D alpha-synuclein transgenic mice were carried out in the animal unit, Royal Free Campus, University College London, London, UK, according to procedures authorized by the UK Home Office. The experimentation involving the alpha-synuclein PFF intrastratial

injection model were approved by Spanish Local Board for Laboratory Animals and performed in accordance with the ethical permission.

### RVG-Exosome Treatment of Mice

For the therapeutic preparation of RVG-exosomes containing shRNA-MCs, 150  $\mu$ g shRNA-MCs and 150  $\mu$ g RVG-exosomes were electroporated (450 V, 100 mA) in 5,000  $\mu$ L electroporation buffer (1.15 mM potassium phosphate [pH 7.2], 25 mM potassium chloride, 21% OptiPrep) and treated with 100 U DNase (Promega) at 37°C for 30 min. After ultracentrifugation (120,000  $\times$  g for 1 h), the exosomes (150  $\mu$ g) were resuspended in 100  $\mu$ L 5% glucose immediately before tail vein injection. Animals were sacrificed 30, 45, or 90 days after injection.

### Clinical Evaluation

To evaluate motor function (see [Supplemental Information](#) for details), mice were tested using the wire hang and negative geotaxis tests. These were conducted before treatment and at 30-day intervals during the study and prior to sacrifice.

### Immunohistochemistry

Animals were perfused with PBS followed by 4% paraformaldehyde in PBS; the brains were post-fixed in 4% paraformaldehyde, cryoprotected in 30% sucrose, frozen, and stored at  $-80^{\circ}\text{C}$ . 30- $\mu$ m-thick coronal sections were prepared using a cryostat. Slices were washed with PBS and were incubated with 3% hydrogen peroxidase in PBS to inactivate the endogenous peroxidase. The slices were washed in PBS and were incubated with a blocking solution (PBS containing 5% normal goat serum, 0.04% Triton X-100) for 1 h. Slices were incubated for 24 or 48 h at 4°C with the primary antibodies ([Table S5](#)): anti-TH (Millipore), anti-alpha-synuclein (phospho S129, Abcam), anti-DAT (Millipore), and anti-Iba1 (Wako). Slices were washed three times with PBS and were then incubated with fluorescent or biotinylated secondary antibody of the appropriate species. All the samples were processed simultaneously to allow comparison.

The total number of DA (TH-positive) neurons in the SNc was estimated by stereological cell counting using the optical fractionator method, which is unaffected by changes in the volume of reference of the structure sampled.<sup>31,32</sup> We used an interactive computer system consisting of an Olympus microscope equipped with a digital camera (Lumenera, MBF Bioscience). The interactive test grids and the motorized stage were controlled by Stereo Investigator software (MicroBrightField Bioscience, Williston, VT, USA). TH-positive stained neurons were counted in the SNc throughout the entire rostrocaudal axis of the SNc (10 sections with a 4-section interval). The total numbers of TH-positive stained neurons in the SNc were calculated using the formula described by West.<sup>33</sup>

Striatal optical density (OD) of TH and DAT immunostaining was used as an index of the density of striatal dopaminergic innervation. This was determined by computer-assisted image analysis using the ImageJ program (NIH, Bethesda, MD, USA). All samples were

processed at the same time, and digital images were captured under the same exposure settings for all experimental analyses. Briefly, six representative rostrocaudal sections (at three levels of the striatum) were examined for each animal, and regions of interest in the striatum were delineated and pixel densities were estimated using ImageJ. Background staining was quantified by measurement of pixel intensities in the white matter and subtracted from striatal regions for normalization.

Numbers of phospho-alpha-synuclein inclusions were manually quantified at 20 $\times$  magnification on coronal sections (120- $\mu$ m intervals between sections) at multiple rostrocaudal levels corresponding to SNc, frontal cortex, striatum, and amygdala from 8 animals per group. SNc aggregates were assessed in sections that covered the full extent of the SNc, double labeled using antibodies against S129 phospho-alpha-synuclein and TH to quantify intra-DA neuron alpha-synuclein inclusions. Aggregates in other regions were quantified in sections stained for S129 phospho-alpha-synuclein. The regions were defined using the Paxinos and Franklin atlas.

For evaluation of microglia activation, representative rostrocaudal sections corresponding to SNc, frontal cortex, striatum, and amygdala were stained with Iba1 antibody (Chemicon). Estimation of numbers of Iba1-positive cells and their average size was calculated using ImageJ software (NIH). Microglial cells were also semiquantitatively analyzed by using a 4-point categorical rating scale developed by Colburn and colleagues,<sup>34</sup> which provides an evaluation of microgliosis based on morphological and immunoreactivity changes. The rating criteria are explained in [Table S6](#).

Immunofluorescent images were captured with a Zeiss LSM 800 confocal scanning laser microscope, and images taken under identical conditions were analyzed with FIJI.

### Western Blot

Cell and brain samples were homogenized in buffer containing: 10 mM Tris/HCl (pH 7.4), 0.1% SDS, protease inhibitor mixture (Thermo Scientific), and DNase (Promega). Samples were solubilized in LDS buffer and reducing agent, separated on NuPAGE Novex 4%–12% Bis-Tris Gels (Invitrogen), blotted onto polyvinylidene fluoride (PVDF) membrane, and analyzed by western blot as previously described<sup>11</sup> using anti-alpha-synuclein (Abcam) and anti-beta-actin (Abcam) antibodies. Horseradish-peroxidase-conjugated anti-mouse immunoglobulin G (IgG) secondary antibody was detected using ECL Western Blot Substrate (Pierce) and Hyperfilm ECL (GE Healthcare). Films were scanned, and signals in the linear range were quantified using ImageJ and normalized to beta-actin levels.

### qPCR

Total RNA was isolated using the RNeasy Kit (QIAGEN) as per the manufacturer's protocol. Reverse transcription (RT) was performed with the qSCRIP Reverse Transcriptase Kit (Primer Design, Southampton, England) as per the manufacturer's instructions. qPCR experiments were performed on the StepOne Real-Time PCR System

(Applied Biosystems) using Precision qPCR Mastermix (Applied Biosystems). Values were calculated using the standard delta-delta Ct method.

### Statistics

Statistical analyses of the data were performed using SPSS, v21.0, using the non-parametric Kruskal-Wallis test and Mann-Whitney U test for *in vitro* experiments and parametric one-way ANOVA followed by the Tukey HSD test or two-tailed t-test for *in vivo* studies.

### SUPPLEMENTAL INFORMATION

Supplemental Information can be found online at <https://doi.org/10.1016/j.ymthe.2019.08.010>.

### AUTHOR CONTRIBUTIONS

J.M.C. and L.A.-E. designed the study. L.A.-E. performed and analyzed cell and transgenic mouse experiments. M.I. and R.F. performed and analyzed alpha-synuclein PFF mouse experiments. J.B. and A.R.-S. performed stereological analysis. S.E. performed the intravenous injections of transgenic mice. R.P. and V.B. synthesized and prepared alpha-synuclein PFFs. R.A.-S. and J.P.S. generated the S129D transgenic mouse model. Y.S. generated the parental alpha-synuclein shRNA plasmid. M. Schleaf and M. Schmeer generated and produced shRNA MCs. C.G. performed the nanoparticle tracking analysis. M.d.T. performed primary and differential analyses of the RNA-seq data. M.I., J.M.C., and L.A.-E. wrote the manuscript. All authors contributed to the manuscript and its amendments.

### CONFLICTS OF INTEREST

L.A.-E. has filed a patent application related to the work in this paper. The remaining authors declare no competing interests.

### ACKNOWLEDGMENTS

The authors would like to thank N. Deglon and J. Agorreta. This study was funded by Parkinson's UK (F-1101 to L.A.-E. and to J.M.C.) and the Michael J. Fox Foundation (15627 to L.A.-E., M.I., and R.F.). This work was supported by the Royal Free London NHS Trust (to R.A.-S. and J.P.S.).

### REFERENCES

- Olanow, C.W., Kieburtz, K., and Katz, R. (2017). Clinical approaches to the development of a neuroprotective therapy for PD. *Exp Neurol* 298, 246–251, Pt. B.
- Simón-Sánchez, J., Schulte, C., Bras, J.M., Sharma, M., Gibbs, J.R., Berg, D., Paisan-Ruiz, C., Lichtner, P., Scholz, S.W., Hernandez, D.G., et al. (2009). Genome-wide association study reveals genetic risk underlying Parkinson's disease. *Nat. Genet.* 41, 1308–1312.
- Lee, V.M., and Trojanowski, J.Q. (2006). Mechanisms of Parkinson's disease linked to pathological alpha-synuclein: new targets for drug discovery. *Neuron* 52, 33–38.
- Li, J.Y., Englund, E., Holton, J.L., Soulet, D., Hagell, P., Lees, A.J., Lashley, T., Quinn, N.P., Rehncrona, S., Björklund, A., et al. (2008). Lewy bodies in grafted neurons in subjects with Parkinson's disease suggest host-to-graft disease propagation. *Nat. Med.* 14, 501–503.
- Kordower, J.H., Chu, Y., Hauser, R.A., Freeman, T.B., and Olanow, C.W. (2008). Lewy body-like pathology in long-term embryonic nigral transplants in Parkinson's disease. *Nat. Med.* 14, 504–506.
- Luk, K.C., Kehm, V., Carroll, J., Zhang, B., O'Brien, P., Trojanowski, J.Q., and Lee, V.M. (2012). Pathological  $\alpha$ -synuclein transmission initiates Parkinson-like neurodegeneration in nontransgenic mice. *Science* 338, 949–953.
- Lewis, J., Melrose, H., Bumcrot, D., Hope, A., Zehr, C., Lincoln, S., Braithwaite, A., He, Z., Ogholikhan, S., Hinkle, K., et al. (2008). In vivo silencing of alpha-synuclein using naked siRNA. *Mol. Neurodegener.* 3, 19.
- Zharikov, A.D., Cannon, J.R., Tapias, V., Bai, Q., Horowitz, M.P., Shah, V., El Ayadi, A., Hastings, T.G., Greenamyre, J.T., and Burton, E.A. (2015). shRNA targeting  $\alpha$ -synuclein prevents neurodegeneration in a Parkinson's disease model. *J. Clin. Invest.* 125, 2721–2735.
- Mingozzi, F., and High, K.A. (2013). Immune responses to AAV vectors: overcoming barriers to successful gene therapy. *Blood* 122, 23–36.
- Alvarez-Erviti, L., Seow, Y., Yin, H., Betts, C., Lakhali, S., and Wood, M.J. (2011). Delivery of siRNA to the mouse brain by systemic injection of targeted exosomes. *Nat. Biotechnol.* 29, 341–345.
- Cooper, J.M., Wiklander, P.B., Nordin, J.Z., Al-Shawi, R., Wood, M.J., Vithlani, M., Schapira, A.H., Simons, J.P., El-Andaloussi, S., and Alvarez-Erviti, L. (2014). Systemic exosomal siRNA delivery reduced alpha-synuclein aggregates in brains of transgenic mice. *Mov. Disord.* 29, 1476–1485.
- Darquet, A.M., Cameron, B., Wils, P., Scherman, D., and Crouzet, J. (1997). A new DNA vehicle for nonviral gene delivery: supercoiled minicircle. *Gene Ther.* 4, 1341–1349.
- Yew, N.S., Zhao, H., Przybylska, M., Wu, I.H., Tousignant, J.D., Scheule, R.K., and Cheng, S.H. (2002). CpG-depleted plasmid DNA vectors with enhanced safety and long-term gene expression in vivo. *Mol. Ther.* 5, 731–738.
- Liu, Y., Li, D., Liu, Z., Zhou, Y., Chu, D., Li, X., Jiang, X., Hou, D., Chen, X., Chen, Y., et al. (2015). Targeted exosome-mediated delivery of opioid receptor Mu siRNA for the treatment of morphine relapse. *Sci. Rep.* 5, 17543.
- Didiot, M.C., Hall, L.M., Coles, A.H., Haraszti, R.A., Godinho, B.M., Chase, K., Sapp, E., Ly, S., Alterman, J.F., Hassler, M.R., et al. (2016). Exosome-mediated delivery of hydrophobically modified siRNA for Huntingtin mRNA silencing. *Mol. Ther.* 24, 1836–1847.
- Kamerkar, S., LeBleu, V.S., Sugimoto, H., Yang, S., Ruivo, C.F., Melo, S.A., Lee, J.J., and Kalluri, R. (2017). Exosomes facilitate therapeutic targeting of oncogenic KRAS in pancreatic cancer. *Nature* 546, 498–503.
- Dehay, B., Bourdenx, M., Gorry, P., Przedborski, S., Vila, M., Hunot, S., Singleton, A., Olanow, C.W., Merchant, K.M., Bezaud, E., et al. (2015). Targeting  $\alpha$ -synuclein for treatment of Parkinson's disease: mechanistic and therapeutic considerations. *Lancet Neurol.* 14, 855–866.
- Joshi, S.N., Butler, D.C., and Messer, A. (2012). Fusion to a highly charged proteosomal retargeting sequence increases soluble cytoplasmic expression and efficacy of diverse anti-synuclein intrabodies. *Mabs* 4, 686–693.
- Moloney, T.C., Hyland, R., O'Toole, D., Paucard, A., Kirik, D., O'Doherty, A., Gorman, A.M., and Dowd, E. (2014). Heat shock protein 70 reduces  $\alpha$ -synuclein-induced predegenerative neuronal dystrophy in the  $\alpha$ -synuclein viral gene transfer rat model of Parkinson's disease. *CNS Neurosci. Ther.* 20, 50–58.
- Spencer, B., Valera, E., Rockenstein, E., Overk, C., Mante, M., Adame, A., Zago, W., Seubert, P., Barbour, R., Schenk, D., et al. (2017). Anti- $\alpha$ -synuclein immunotherapy reduces  $\alpha$ -synuclein propagation in the axon and degeneration in a combined viral vector and transgenic model of synucleinopathy. *Acta Neuropathol. Commun.* 5, 7.
- Tran, H.T., Chung, C.H.-Y., Iba, M., Zhang, B., Trojanowski, J.Q., Luk, K.C., and Lee, V.M.Y. (2014).  $\alpha$ -synuclein immunotherapy blocks uptake and templated propagation of misfolded  $\alpha$ -synuclein and neurodegeneration. *Cell Rep.* 7, 2054–2065.
- Zhao, H.T., John, N., Delic, V., Ikeda-Lee, K., Kim, A., Weihofen, A., Swayze, E.E., Kordasiewicz, H.B., West, A.B., and Volpicelli-Daley, L.A. (2017). LRRK2 antisense oligonucleotides ameliorate  $\alpha$ -synuclein inclusion formation in a Parkinson's disease mouse model. *Mol. Ther. Nucleic Acids* 8, 508–519.
- Kim, Y.C., Miller, A., Lins, L.C., Han, S.W., Keiser, M.S., Boudreau, R.L., Davidson, B.L., and Narayanan, N.S. (2017). RNA interference of human  $\alpha$ -synuclein in mouse. *Front. Neurol.* 8, 13.

24. Benskey, M.J., Sellnow, R.C., Sandoval, I.M., Sortwell, C.E., Lipton, J.W., and Manfredsson, F.P. (2018). Silencing alpha synuclein in mature nigral neurons results in rapid neuroinflammation and subsequent toxicity. *Front. Mol. Neurosci.* *11*, 36.
25. Gorbatyuk, O.S., Li, S., Nash, K., Gorbatyuk, M., Lewin, A.S., Sullivan, L.F., Mandel, R.J., Chen, W., Meyers, C., Manfredsson, F.P., and Muzyczka, N. (2010). In vivo RNAi-mediated alpha-synuclein silencing induces nigrostriatal degeneration. *Mol. Ther.* *18*, 1450–1457.
26. Xhima, K., Nabbouh, F., Hynynen, K., Aubert, I., and Tandon, A. (2018). Noninvasive delivery of an  $\alpha$ -synuclein gene silencing vector with magnetic resonance-guided focused ultrasound. *Mov. Disord.* *33*, 1567–1579.
27. Abeliovich, A., Schmitz, Y., Fariñas, I., Choi-Lundberg, D., Ho, W.H., Castillo, P.E., Shinsky, N., Verdugo, J.M., Armanini, M., Ryan, A., et al. (2000). Mice lacking alpha-synuclein display functional deficits in the nigrostriatal dopamine system. *Neuron* *25*, 239–252.
28. Klivenyi, P., Siwek, D., Gardian, G., Yang, L., Starkov, A., Cleren, C., Ferrante, R.J., Kowall, N.W., Abeliovich, A., and Beal, M.F. (2006). Mice lacking alpha-synuclein are resistant to mitochondrial toxins. *Neurobiol. Dis.* *21*, 541–548.
29. Gelders, G., Baekelandt, V., and Van der Perren, A. (2018). Linking neuroinflammation and neurodegeneration in Parkinson's disease. *J. Immunol. Res.* *2018*, 4784268.
30. Duffy, M.F., Collier, T.J., Patterson, J.R., Kemp, C.J., Luk, K.C., Tansey, M.G., Paumier, K.L., Kanaan, N.M., Fischer, D.L., Polinski, N.K., et al. (2018). Lewy body-like alpha-synuclein inclusions trigger reactive microgliosis prior to nigral degeneration. *J. Neuroinflammation* *15*, 129.
31. Gonzalez-Reyes, L.E., Verbitsky, M., Blesa, J., Jackson-Lewis, V., Paredes, D., Tillack, K., Phani, S., Kramer, E.R., Przedborski, S., and Kottmann, A.H. (2012). Sonic hedgehog maintains cellular and neurochemical homeostasis in the adult nigrostriatal circuit. *Neuron* *75*, 306–319.
32. Kett, L.R., Stiller, B., Bernath, M.M., Tasset, I., Blesa, J., Jackson-Lewis, V., Chan, R.B., Zhou, B., Di Paolo, G., Przedborski, S., et al. (2015).  $\alpha$ -Synuclein-independent histopathological and motor deficits in mice lacking the endolysosomal Parkinsonism protein Atp13a2. *J. Neurosci.* *35*, 5724–5742.
33. West, M.J. (1993). New stereological methods for counting neurons. *Neurobiol. Aging* *14*, 275–285.
34. Colburn, R.W., DeLeo, J.A., Rickman, A.J., Yeager, M.P., Kwon, P., and Hickey, W.F. (1997). Dissociation of microglial activation and neuropathic pain behaviors following peripheral nerve injury in the rat. *J. Neuroimmunol.* *79*, 163–175.